PHYSICAL REVIEW A VOLUME 37, NUMBER 3 FEBRUARY 1, 1988

Smectic-C "chevron," a planar liquid-crystal defect: Implications for the surface-stabilized ferroelectric liquid-crystal geometry

N. A. Clark and T. P. Rieker
Department of Physics, Condensed Matter Laboratory, and Center for Optoelectronic Computing Systems, University of Colorado, Boulder, Colorado 80309
(Received 12 June 1987)

The recent discovery of "chevron" structured smectic-*C* (SC) layers in surface-stabilized ferroelectric liquid-crystal (SSFLC) cells [T. P. Rieker, N. A. Clark, G. S. Smith, D. S. Parmar, E. B. Sirota, and C. R. Safinya, Phys. Rev. Lett. **59**, 2568 (1987)] enables the understanding of many commonly observed features of SSFLC director and layer structure. We present the full three-dimensional layer structure of zigzag walls, the predominant SSFLC defect, which we find to mediate change in chevron direction. We show that stabilization of the director field in SC chevron cells occurs at the chevron interface, so that SC chevron cells behave as two nearly independent cells optically and electrically in series.

Liquid crystals (LC's) are characterized by a wide variety of defects wherein order parameters such as the director field $\hat{\mathbf{n}}$, giving the mean local molecular orientation, exhibit singular behavior along lines or points.[1] The "chevron" defect,[2] is the first example to be found of the class of planar LC defects, in which the order parameter discontinuities occur at a planar sheet, parallel to which there is *full* translational invariance. In a chevron, the planar smectic-*C* (SC) layers reorient as they cross the defect ($x=0$) plane in a mirror-symmetric way, such that, referring to Fig. 1(a), $\hat{\mathbf{s}}_+\cdot\hat{\mathbf{z}}=\hat{\mathbf{s}}_-\cdot\hat{\mathbf{z}}=\cos\delta$. SC chevrons are found in cells prepared by cooling from the smectic-*A* (SA) in a micron dimension gap between solid plates.[2]

The chevron interface ($x=0$) significantly influences the orientational structure of the director field $\hat{\mathbf{n}}(\mathbf{r})$ and polarization $\mathbf{P}(\mathbf{r})=P_0(\hat{\mathbf{s}}\times\hat{\mathbf{n}})$ in its vicinity. Figure 1(a) shows the tilt cones with directors $\hat{\mathbf{n}}_+$ and $\hat{\mathbf{n}}_-$ giving the orientations ϕ_+ and ϕ_- immediately adjacent to the chevron interface. If the angle δ satisfies the condition $\delta<\theta$, then the + and − cones intersect at the open circles U (up) and D (down) in Fig. 1(a), and adjusting ϕ_+ and ϕ_- to either of these intersections makes the orientation of $\hat{\mathbf{n}}$ everywhere uniform and parallel to the chevron interface plane. This condition and the layer tilt thus produce pretilt of the polarization in accord with arguments of Handschy and Clark,[3] with pretilt changing sign as the chevron is crossed (Fig. 1). In these minimum energy states, the chevron elastic energy will arise from the Frank-type elasticity resisting abrupt change of the SC biaxial order parameter, i.e., reorientation of the (SC tilt) plane locally containing $\hat{\mathbf{s}}$ and $\hat{\mathbf{n}}$ [dashed lines in Fig. 1(a)]. Assuming an elastic constant L for this reorientation, and a layer compression elastic constant B, then dx, the width in x of the chevron tip, will be determined by the competition of orientational and compressional forces to be $dx\approx L/B\delta\lesssim 100$ Å. We thus expect the chevron reorientation to be abrupt.

The application of an electric field and/or the boundary conditions at the solid surfaces will in general lead to gradients in ϕ and consequent torques tending to move ϕ_+ and ϕ_- from U or D. For a given ϕ_- the interface orientational elastic energy will be minimized by that ϕ_+ which satisfies the equation

$$\cos(2\delta)\cos(\phi_-)\sin(\phi_+)+\sin(\phi_-)\cos(\phi_+)+\sin(2\delta)\cos(\theta)=0\ ,$$

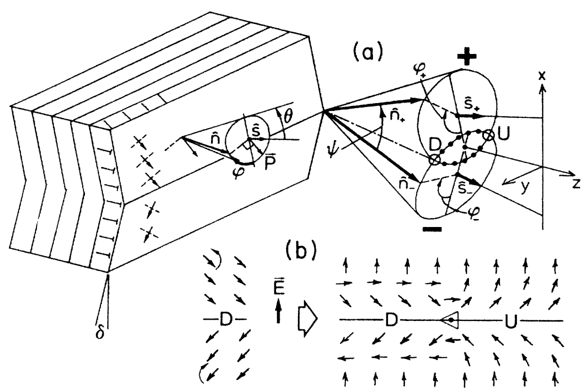

FIG. 1. Geometry of the director field at a smectic-*C* chevron interface. (a) The SC is a locally biaxial structure of liquid-like layers in which $\hat{\mathbf{n}}(\mathbf{r})$ is tilted at an equilibrium angle θ relative to the local layer normal $\hat{\mathbf{s}}(\mathbf{r})$ and is free to reorient azimuthally through the angle ϕ on a cone of axis $\hat{\mathbf{s}}$. Subscripts + and − refer to quantities on opposite sides of the chevron. For $\delta<\theta$, the cone intersections U and D (open circles) are the equilibrium orientations of $\hat{\mathbf{n}}$, having $\hat{\mathbf{n}}$ parallel to the interface. In these states the FLC polarization $\mathbf{P}$ is pretilted such that starting from the D state and applying a field $\mathbf{E}$ along $\hat{\mathbf{x}}$, the polarizations rotate in opposite directions on opposite sides of the chevron, moving along the dotted paths from D to U for sufficiently large E. (b) At lower E, reorientation at the chevron interface occurs via motion of the domain wall trapped in the chevron interface plane terminating the 2π disclination which is also trapped at the chevron interface by $\mathbf{E}$.

obtained from minimizing the angle ψ $(\theta,\delta,\phi_+,\phi_-)$ between $\hat{\mathbf{n}}_+$ and $\hat{\mathbf{n}}_-$. The key feature of this geometry is that, for δ comparable to θ, the physically relevant condition, $|\phi_+|<\phi_{\max}$, that is, ϕ_+ varies over a finite range for a complete 2π rotation of ϕ_-. In this case ϕ_+ can be decoupled from ϕ_- with application of torque large enough to overcome an orientational energy barrier of at most $\gamma \sim (K/dx)(\psi_{\max})^2 \sim (K/dx)(2\delta)^2 \sim 2\times 10^{-2}$ ergs/cm^2, where K is a typical nematic Frank constant. This barrier is comparable to typical LC–solid-surface interaction energies.[4]

The energy barrier for the decoupling of ϕ_+ and ϕ_- is in fact much lower in one situation of crucial importance, namely, the response of the director to applied electric field **E**. The change of pretilt sign at the chevron leads to opposite signs of rotation in ϕ on opposite sides of the chevron [Fig. 1(b)], producing in response to sufficiently high **E** a transition from the D to U state in which n_+ and n_- rotate on the dotted paths ($\cdots$) from D to U in Fig. 1(a). The surface energy maximum for this D to U reorientation, $\gamma_{DU} \sim (K/dx)(\delta-\phi)^2$, is much less than γ when $\delta \sim \theta$. For E's exerting a torque density larger than γ_{DU}, n_+ and n_- homogeneously decouple, the D to U transition occurring without domain walls (high-field limit[3]). At lower **E** the opposite rotation sense above and below the chevron traps at the chevron interface plane a 2π disclination sheet in ϕ. The chevron-associated pretilt conditions thus account for the internal disclination identified by Ouchi *et al.*[5] Holes nucleating in this 2π sheet, shown in Fig. 1(b), are the domain loops observed in strobe microscopy experiments.[6,5] These internal disclination loops are trapped in the chevron interface planes and move in these planes. This can be observed directly by noting that, in cells with asymmetric chevrons (see Fig. 2 and Ref. 1), the domain loops in a given region remain in fixed planes normal to x and have the same plane of focus as the chevron plane, determined as discussed below.

We have a variety of other evidence for this internal surface orientational energy barrier. For example, referring to Figs. 2(a)–2(c), it is well known that if a surface-stabilized ferroelectric liquid-crystal (SSFLC) cell is sufficiently thick that the bulk ferroelectric liquid-crystal (FLC) helix will appear, along with disclination (dechiralization) lines which allow it to coexist with a fixed orientation at the bounding surface.[7] In a chevron cell as the thickness is increased two sets of dechiralization lines will appear, one set in each branch of the chevron.

SSFLC cells, when viewed in transmission polarized light microscopy, show a variety of characteristic features in their optical texture. The most striking and prevalent of these are the so-called zigzag defects,[3,5] consisting of narrow walls running almost along $\hat{\mathbf{z}}$ [Figs. 2(d) and 2(e)] and broad walls running normal to $\hat{\mathbf{z}}$ [Figs. 2(f) and 2(e)]. In thicker SC cells ($d>3$ μm) these walls separate regions of uniform but different optical contrast, an observation which led us to suggest that zigzag walls separated regions of different tilt of the layers relative to the bounding plates.[3] Our discovery of the chevron layer structure and subsequent microscopy has enabled us to build a detailed three-dimensional structural model for the zigzag defect walls, which is shown in Fig. 2(e).

The chevron formation in the SC spontaneously breaks the SA mirror symmetry normal to $\hat{\mathbf{z}}$ and causes the SC to be a mosaic of two kinds of domains, each having one of the two possible chevron directions. Zigzag defects are the spontaneously formed boundaries between domains having taken opposite chevron directions. This confirms the proposal initially made by Handschy and Clark[3] that zigzag walls in SSFLC cells separate regions of differing layer tilt. That is, moving along $\hat{\mathbf{z}}$ and crossing a narrow zigzag wall the chevrons change direction, pointing out from the defect as follows: $\langle\langle\langle\langle\langle\rangle\rangle\rangle\rangle\rangle$. The broad wall of the defect running parallel to the layers mediates the opposite change: $\rangle\rangle\rangle\rangle\rangle\langle\langle\langle\langle\langle$. This aspect of the structure results in the simple topology that as one moves in a cell parallel to $\hat{\mathbf{z}}$, one alternately encounters narrow and then broad lines.

We propose that the remarkable structure of these defects is a result of the same simple conditions that produce the chevron in the first place:[2] (1) the layers are anchored in the SA phase with a pitch p (length along $\hat{\mathbf{z}}$ per layer)$=d_A$ and this anchoring persists into the SC phase which, as a result, must also have $p=d_A$, but with thinner layers ($d_C<d_A$); (2) the accommodation of $p=d_A$ is achieved via the tilt of continuous layers. *The model of Fig. 2(e) is a structure which mediates the switch in chevron direction while satisfying the above conditions.*

Figure 2(g) shows an *x*-*z* section of the layering structure through the defect in case of symmetric chevrons ($\delta_A=0$).[2] The chevrons achieve $p=d_A$ by rotating the layers about $\hat{\mathbf{y}}$ through the tilt angle $\delta_C=\cos^{-1}d_C/d_A$. In making the $\langle\langle\langle\langle\langle$:::$\rangle\rangle\rangle\rangle\rangle$ (narrow wall) transition, the layers must be effectively thicker near the chevron plane in the transition region (:::). This is achieved by rotating the layers away from being normal to $\hat{\mathbf{z}}$ through an angle slightly larger than δ_C. In order to mediate the chevron direction change this rotation must be about $\hat{\mathbf{x}}$ rather than $\hat{\mathbf{y}}$. The very simple continuous layer structure shown in Figs. 2(e) and 2(h), having a parallelogram-shaped planar element to mediate the chevron sign switch, results. The limits of the zigzag wall, which focus as sharp lines in the polarized light microscope [Fig. 2(d)], are the lines formed by the loci of points where the chevron planes intersect the parallelogram in successive SC layers, indicated by the heavy solid and dashed lines in Fig. 2(e). The tendency for the narrow part of the zigzag walls to run at a small angle relative to $\hat{\mathbf{z}}$ is a result of the corresponding asymmetry in the stacking of the parallelograms in successive layers. At the "tips," where narrow walls meet, the two defects merge in a continuous way [Fig. 2(e)].

In making the $\rangle\rangle\rangle\rangle\rangle$:::$\langle\langle\langle\langle\langle$ (broad wall) transition, the layers must be effectively thinner near the chevron plane in the transition region. This is achieved by rotating the layers through an angle less than δ_C, inside a right parallelogram cylinder running parallel to y. The limits of this cylinder, indicated by the heavy solid and dashed lines in Fig. 2(e), are the visible limits of the broad wall in Fig. 2(f). In the case of asymmetric chevrons, the lines on one side of a zigzag wall focus near the top of the cell and those on the other side near the bottom, as would be expected from Fig. 2(e). At the center of the broad wall, the layers have their maximum thickness without a chevron [Fig. 2(e)], making this region the most favorable for forming dechiralization lines [Fig. 2(f)].

Further direct evidence for this model, obtained with the polarized light microscope is shown in Figs. 2(h) and 2(j). With a 5 to 10-μm-thick cell it is possible to obtain zigzag defects crossed by dechiralization lines. This is quite useful as the dechiralization lines dress the FLC layering structure, running along the boundaries of the wide planar element of an asymmetric chevron [Fig. 2(h)], enabling it to be directly observed. Figures 2(i) and 2(j) show a typical result, with lines on opposite

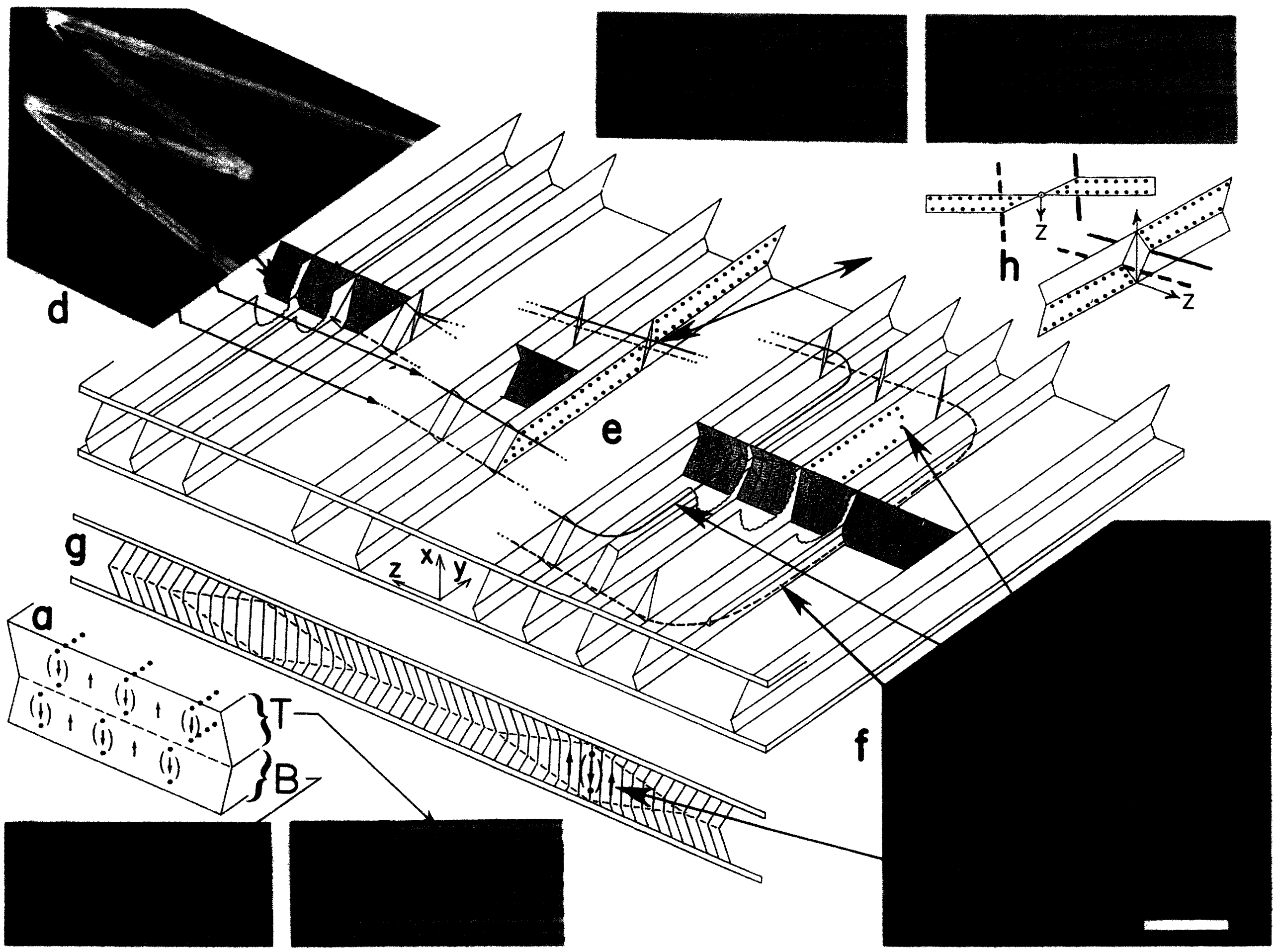

FIG. 2. (a) In sufficiently thick cells, a director constraint at the chevron should lead to independent dechiralization lines [indicated throughout the figure by the heavy dotted lines (· · ·)] appearing on either side of the chevron defect. (b) and (c) Photomicrographs obtained in polarized transmission microscopy of dechiralization lines in a 6-μm-thick SSFLC cell, focusing near the top and bottom, respectively, of the FLC cell, showing the two sets of lines. (d) and (f) Photomicrographs of the narrow and broad walls of zigzag defects in 3 to 4-μm-thick cells, respectively. (e) The three-dimensional structure of a closed zigzag defect loop, the spontaneously formed defect separating one direction of chevron from the other in a SC formed between solid plates by cooling from the SA. The loop consists of narrow walls running nearly parallel to $\hat{z}$ and a broad wall running parallel to $\hat{y}$. These walls are delimited by the lines which focus sharply in (d) and (f), which are also indicated by the heavy solid and dashed lines in (e). In this example the mean layer tilt is nonzero [asymmetric chevron (Ref. 2)]. The defect structure is characterized by a construction of layers made up of planar elements, continuously connected to one another by the chevron discontinuities of Fig. 1. Thus *all of the solid lines on the layers are chevron discontinuities.* The overall structure maintains *everywhere* the mean layer pitch $p = d_A$ established by layer anchoring in the SA phase (no dislocations required). (g) Section showing layer structure change upon passing through the narrow (⟨⟨⟨⟩⟩⟩) and broad (⟩⟩⟩⟨⟨⟨) walls for the symmetric case. Upon reduction of an electric field, dechiralization lines first appear in the center of the broad wall, where the layers are chevron free [(e),(f),(g)]. (h) Dechiralization lines dress the layer structure near a narrow zigzag wall, outlining the limits of the wider chevron element. (i) and (j) Photos of dechiralization lines crossing zigzag defects in a 5-μm-thick cell, focused near the top and bottom, respectively, of the FLC cell. The lines on opposite sides of the zigzag wall focus at different x values, as expected from (h). All photos were made using a Zeiss Universal microscope with a UD condenser and an Epiplan 40X objective observing a 50%-50% W7-W82 mixture (Ref. 2). The bar in (f) is 15 μm long.

sides of a narrow wall focusing at different x values.

The geometry of $\hat{\mathbf{n}}$ at the chevron interface and solid surfaces leads to a basic requirement for obtaining bistability in SSFLC cells: One must have $\theta > \delta$.[8] Since $\delta = \arccos(d_C/d_A)$ is determined solely by the bulk material property d_C/d_A, bistability *requires* that the bulk condition $\cos\theta > d_C/d_A$ be satisfied by the material being employed. That is, the smectic-C layer thickness *must be larger* than $d_A\cos\theta$ which would be obtained in a model of sticklike molecules being tilted over. In fact, most smectic-C materials where this condition has been measured have $\cos\theta > d_C/d_A$,[9] but there are definite exceptions.[10]

This work was supported by the U.S. Army Research Office, Contract No. DAAL03-86-K-0053 and the National Science Foundation, Grant No. CDR 8622236.

[1]M. Kleman, *Points, Lines, and Walls* (Wiley, New York, 1981).

[2]T. P. Rieker, N. A. Clark, G. S. Smith, D. S. Parmar, E. B. Sirota, and C. R. Safinya, Phys. Rev. Lett. **59**, 2568 (1987).

[3]M. A. Handschy and N. A. Clark, Ferroelectrics **59**, 69 (1984).

[4]J. Cognard, Mol. Cryst. Liq. Cryst., Supplement **1** (1982).

[5]Y. Ouchi, H. Takazoe, and A. Fukuda, Jpn. J. Appl. Phys. **26**, 1 (1984).

[6]M. A. Handschy and N. A. Clark, Appl. Phys. Lett. **41**, 39 (1982).

[7]M. Brunet and C. Williams, Ann. Phys. (Paris) **3**, 237 (1978).

[8]N. A. Clark and S. T. Lagerwall, Ferroelectrics **59**, 25 (1984).

[9]C. R. Safinya, M. Kaplan, J. Als-Nielsen, R. J. Birgenau, D. Davidov, and J. D. Litster, Phys. Rev. B **21**, 4149 (1980); E. N. Keller, E. Nachaliel, and D. Davidov, Phys. Rev. A **34**, 4363 (1986).

[10]B. M. Ocko, A. R. Kortan, R. J. Birgenau, and J. W. Goodby, J. Phys. (Paris) **45**, 113 (1984).

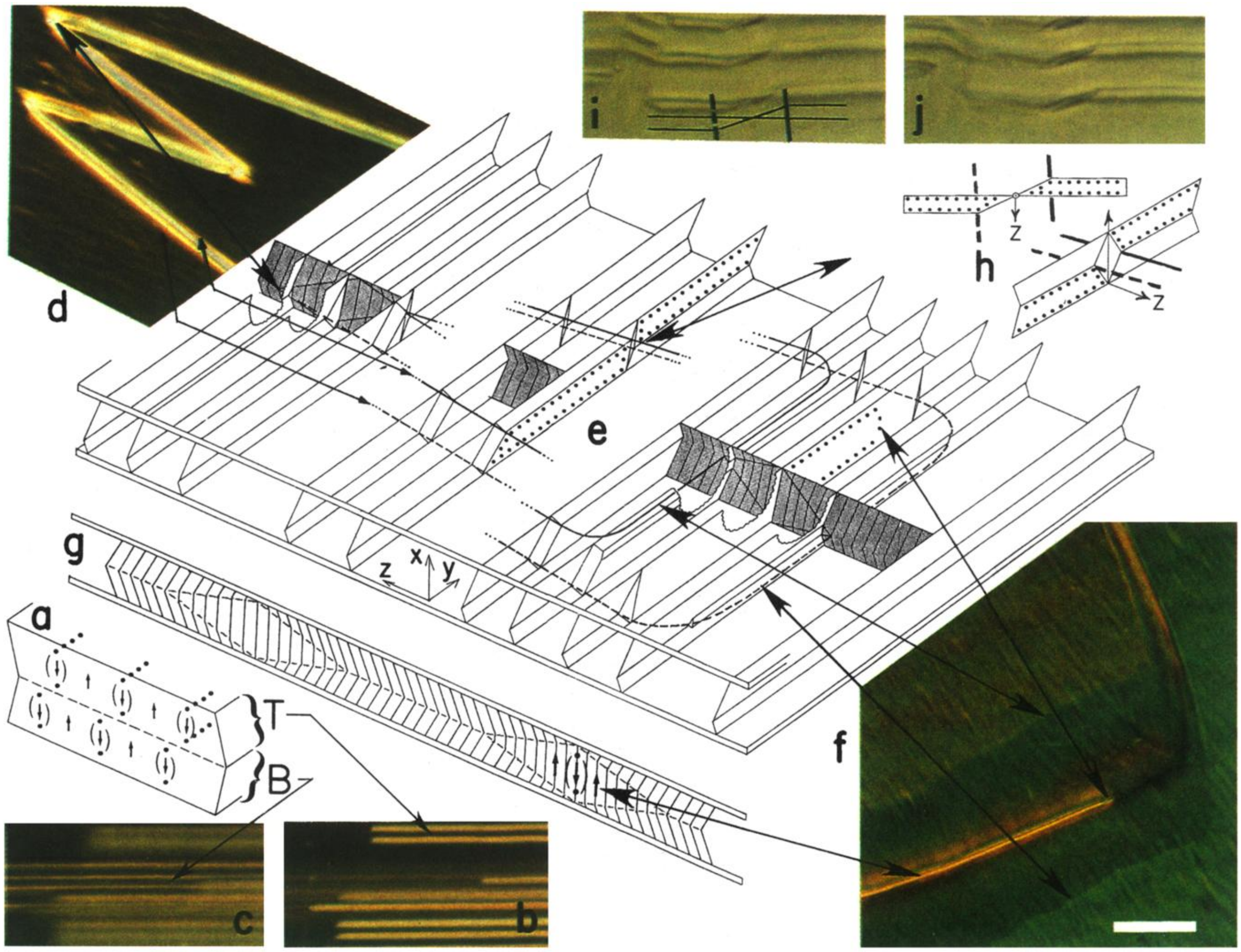

FIG. 2. (a) In sufficiently thick cells, a director constraint at the chevron should lead to independent dechiralization lines [indicated throughout the figure by the heavy dotted lines (· · ·)] appearing on either side of the chevron defect. (b) and (c) Photomicrographs obtained in polarized transmission microscopy of dechiralization lines in a 6-μm-thick SSFLC cell, focusing near the top and bottom, respectively, of the FLC cell, showing the two sets of lines. (d) and (f) Photomicrographs of the narrow and broad walls of zigzag defects in 3 to 4-μm-thick cells, respectively. (e) The three-dimensional structure of a closed zigzag defect loop, the spontaneously formed defect separating one direction of chevron from the other in a SC formed between solid plates by cooling from the SA. The loop consists of narrow walls running nearly parallel to $\hat{\mathbf{z}}$ and a broad wall running parallel to $\hat{\mathbf{y}}$. These walls are delimited by the lines which focus sharply in (d) and (f), which are also indicated by the heavy solid and dashed lines in (e). In this example the mean layer tilt is nonzero [asymmetric chevron (Ref. 2)]. The defect structure is characterized by a construction of layers made up of planar elements, continuously connected to one another by the chevron discontinuities of Fig. 1. Thus *all of the solid lines on the layers are chevron discontinuities.* The overall structure maintains *everywhere* the mean layer pitch $p = d_A$ established by layer anchoring in the SA phase (no dislocations required). (g) Section showing layer structure change upon passing through the narrow (⟨⟨⟨⟩⟩⟩) and broad (⟩⟩⟩⟨⟨⟨) walls for the symmetric case. Upon reduction of an electric field, dechiralization lines first appear in the center of the broad wall, where the layers are chevron free [(e),(f),(g)]. (h) Dechiralization lines dress the layer structure near a narrow zigzag wall, outlining the limits of the wider chevron element. (i) and (j) Photos of dechiralization lines crossing zigzag defects in a 5-μm-thick cell, focused near the top and bottom, respectively, of the FLC cell. The lines on opposite sides of the zigzag wall focus at different x values, as expected from (h). All photos were made using a Zeiss Universal microscope with a UD condenser and an Epiplan 40X objective observing a 50%-50% W7-W82 mixture (Ref. 2). The bar in (f) is 15 μm long.